

# Relaxed Steering towards Oriented Region Goals

Ronan Boulic

VRLAB, Ecole Polytechnique Fédérale de Lausanne, EPFL  
1015 Lausanne, Switzerland  
Ronan.Boulic@epfl.ch  
<http://vrlab.epfl.ch>

**Abstract.** This paper extends the *funnelling* behavior to offer a low-cost flexible guidance of mobile entities towards a circular region goal with the guarantee of enforcing an orientation within a predefined tolerance interval. The key requirements are the same as the funnelling control, i.e. a low and constant cost update of the control even when the goal parameters change (distance and relative orientation of the goal, position tolerance radius, orientation tolerance interval, desired speed). The smoothness and the optimality of the resulting trajectory being of high importance the paper qualitatively compares the trajectories produced by both funnelling algorithms. The new relaxed approach appears to produce smoother and shorter path for path made of a succession of large region goals. These qualities and its low cost advocate for its exploitation for moving through large dynamically changing regions without precise a priori planning.

## 1 Introduction

Despite describing a large repertoire of steering behaviors, the key paper from Reynolds [R99] does not offer a method for reaching a target position with a prescribed orientation. A fast controller achieving such a funnelling behavior has been introduced in [B05a,b] as illustrated in Fig. 1 that compares trajectories for reaching a target position (red circle) without (left) and with a prescribed orientation  $\beta$  (right). At its core lies a simple *seek* Proportional-Derivative orientation controller aiming at zeroing the orientation error  $\alpha$  between the forward direction and the radial direction

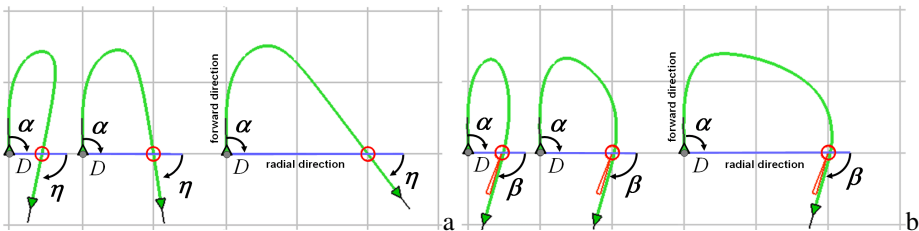


**Fig. 1.** : (a) reaching three position goals with a “seek” controller, (b) reaching the same position with a prescribed final orientation  $\beta$  with a *funnelling* controller [B05a,b]

linking the current position to the desired position (Fig. 1 left). The funnelling behavior modulates the goal of the seek controller to achieve the desired orientation  $\beta$ .

The next section briefly situates this approach with respect to prior efforts in gait trajectory control for crowds with an emphasis on collision avoidance.

## 2 Background

Reynolds achieves collision avoidance in [R99] first by extrapolating the trajectory as a straight line; in a second stage a repulsive behavior is exploited whenever the extrapolated trajectory intersects an obstacle. This is generalized for multiple moving entities; it results in a combination of turning away and accelerating/decelerating depending on the relative location of colliding entities [R00]. An especially demanding class of moving entities requesting finely tuned steering behaviors is the Robot-Cup soccer agent described in [BOM03]. This work stresses limitation of the Seek behavior such as getting trapped in local orbital minima and oscillations. Another important class of characters is pedestrians; Helbing and Molnar have reproduced the motion of pedestrian groups in some well-known contexts (e.g. corridor) by subjecting them to “social forces” resulting from the combination of potential fields [HM95]. Raup-Musse and Thalmann have exploited Bézier curves to introduce some variety in groups’ behavior within a crowd [R01]; collision avoidance is handled through the intersection of predicted linear trajectories. A similar approach of collision avoidance is adopted by Lamarche and Donikian [LD04]. Metoyer and Hodgins have associated potential fields to user-supplied natural path and proposed a higher level management of pedestrian collision avoidance [MH04]. Brogan and Johnson have built a walking path model from measurements from which they construct a heading chart ensuring trajectories with minimal radius of curvature towards a goal while avoiding static obstacles [BJ03]. Another approach based on measured data is described in [PPD07] where two subjects modify their trajectories to avoid colliding into each other. A model is derived for controlling walking agents in a crowd.

A planning approach exploiting probabilistic roadmaps is described in [P08]; the approach allows to prevent collisions between a moving human body and a complex static environment. A partial planning approach is proposed in Go et al. [GTK06]; it offers a good compromise between the reactivity to a dynamic environment and local minima avoidance. These authors pre-calculate 3D trajectory segments in a local coordinate system for a sampling of various initial conditions; this high precision prediction is made for the principal mobile entity while the prediction made for other mutually dependent vehicles exploit a linear extrapolation

The trajectories produced with the funneling behavior [B05a] show high similarities with the experimental trajectories studied in [ALHB06]. A comparison with Bezier curves highlights that their local curvature near the destination appears to be independent of the distance for distances over 4 meters [B05b]. The present paper examines how to relax the funnelling control so as to fully take advantage of the concept of *region goal*, for which any point of the region is equally valid as temporary goal. This kind of region goals can easily be inferred from higher level planning data structures such as the graph from [P08] or the corridors from [GKKO08]. We show

that such an approach produces smoother and shorter paths than the standard funneling approach. In the longer term we adhere to the idea of steering benchmarks that include not only relaxed funnelling reaches as described here but also more complex scenarios involving a higher management level for collision avoidance [SNKFR08].

The paper first illustrates the key concepts behind the standard funnelling approach and highlights the comparison with human trajectories. We then stress the limitation of the concept of position tolerance when exploited in that framework. The principle of the relaxed funnelling is then presented in details. Various case studies compare both algorithm prior to report on their relative computing cost. The conclusion summarizes the various advantages introduced by the relaxed funnelling and suggests future directions of researches.

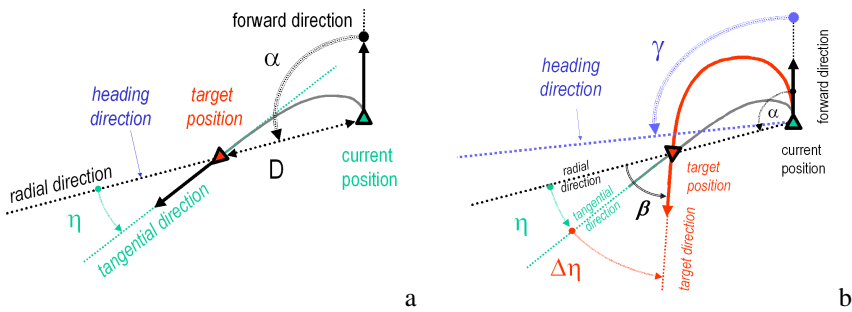


**Fig. 2.** (a) the radial direction is the heading direction for the seek controller, (b) funneling controller modulating the heading direction to achieve a target orientation

### 3 The Standard Funnelling Controller

The seek controller we exploit is different from the one proposed in [R99] as we prevent high angular and normal accelerations. The radial direction (Fig. 2a) is considered as the desired heading direction to be achieved by the mobile entity. One key angle to notice is the angle  $\eta$  made by the tangential direction at the target with the initial radial direction ; it is pre-computed for an anisotropic polar sampling of position goals (Fig 3a). The *funnelling* controller modulates the desired heading direction so that a desired final orientation  $\beta$  is finally achieved at the target position (Figure 2b). The modulation is a function of the angular difference  $\Delta\eta = \beta - \eta$  between the desired direction  $\beta$  and the tangential direction  $\eta$  that would be obtained with the sole seek controller. This angle error  $\Delta\eta$  is almost the only input for updating the angular acceleration ; it requests only to interpolate the  $\eta$  angle from the pre-computed table. In a second stage we ensure the convergence of the control algorithm by computing an upper limit for the quantity  $(-\Delta\eta)$  applied to the desired heading direction. The result is the *modulated heading direction*  $\gamma$  that is provided as instantaneous goal to the plain seek controller (Figure 2b).

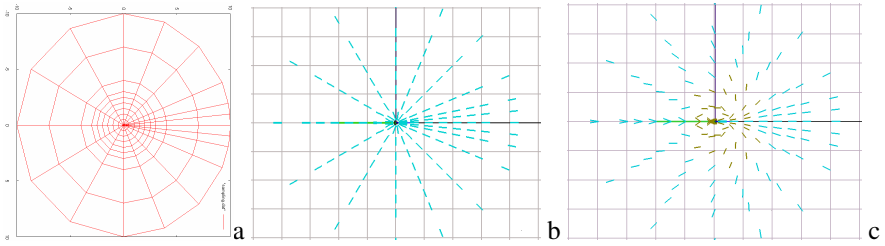


**Fig. 3.** (a) Anisotropic polar sampling for precomputing the  $\eta$  angle : the horizontal axis is oriented along the forward direction of the mobile entity. Central region of the local funnelling field build from the precomputed  $\eta$  angles for slow (b) and normal (c) linear velocities (null angular velocity in both cases). The darker colour around the mobile entity in (c) indicates that the corresponding sampled target could not be reached with the default seek controller [B05a]; the  $\eta$  angle obtained successfully for a smaller desired velocity is stored and displayed instead.

Conceptually the funnelling approach can be viewed as a field-driven steering approach. A major difference with other approaches relying on vector fields for steering is that our field is expressed in the local coordinate system of the mobile entity. Moreover the stored  $\eta$  angle for each sampled goal (Fig 3a) is a function of three variables, namely the current linear and angular velocities and the desired linear velocity. This explains the displayed variations between Fig.3 b (slow linear velocities) and Fig. 3c

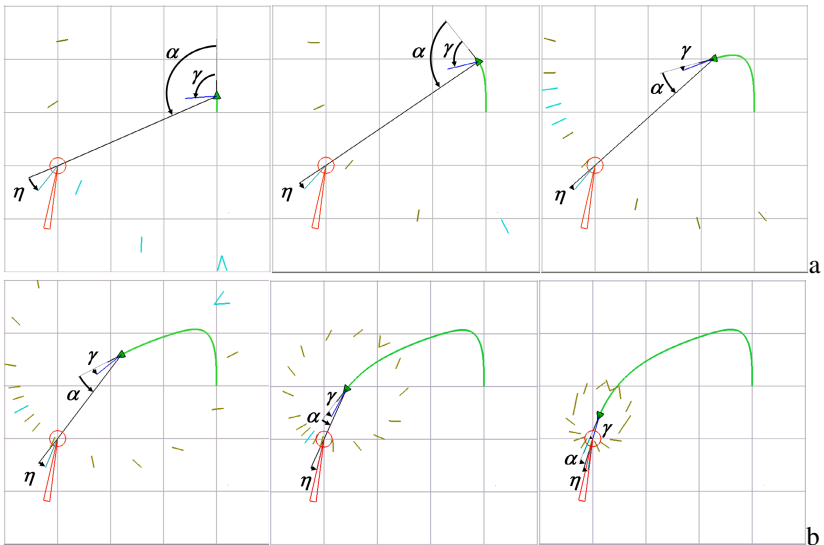


**Fig. 4.** (a  $\rightarrow$  b, left to right) examples of states extracted from the trajectory of a case similar to Fig2b where the target location and orientation are indicated by their respective tolerances with a circle and a triangle. Also visible are the current radial direction in black, the interpolated  $\eta$  angle at the target location, the modulated heading direction  $\gamma$  at the current location and the closest\_distance ring of the local field.

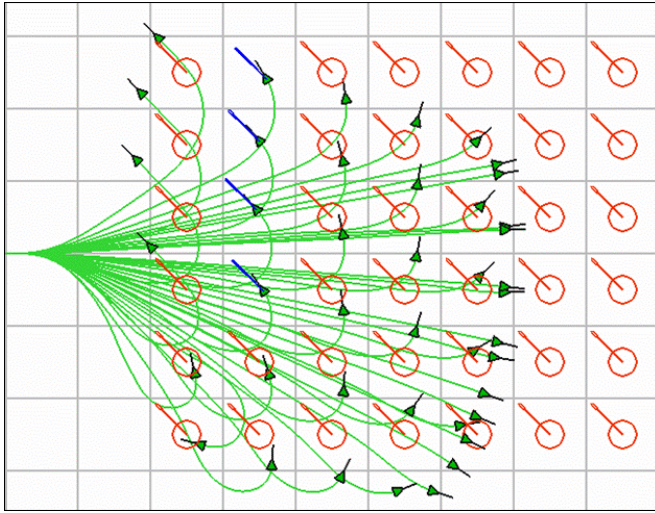


**Fig. 5.** Funnelling trajectories replicating human gait trajectories measured in [ALHB06]

(normal desired linear velocities). In the first case the final tangential directions appear to be oriented radially (Fig. 3b) whereas this is only the case for sampled goals lying in front of the mobile entity for Fig.3 c.

Fig. 4 a,b show both  $\eta$  and  $\gamma$  angles displayed for states extracted from a case analog to the one of Fig2. b. Only one ring of the local vector field is displayed for clarity purpose. In that example the initial and desired linear velocities have mid-range values. More trajectories resulting from the funnelling control are shown on Fig.5. All have the same initial state and desired global orientation but distinct target locations. This case corresponds to one case of the experimental protocol used in [ALHB06] for measuring human gait trajectories. The simulated funnelling trajectories offer high similarities with those captured [ALHB06]. For more details on the standard funnelling see [B05a,b].

#### 4 Funnelling towards a Region Goal

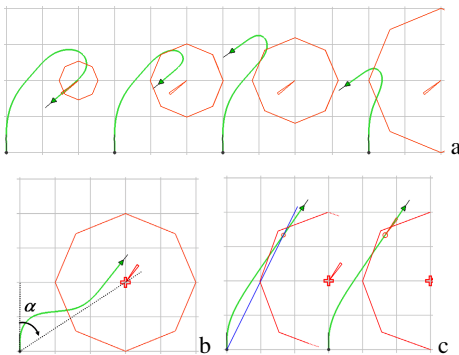


**Fig. 6.** Relaxed steering, (a) (b) with a tolerance, (c) sampled goal with smallest  $\Delta\eta$

Defining a tolerance around the desired position (red circle) allows to relax the steering to a pure direction control once the position tolerance is met (Fig. 6a). However in these examples the  $\alpha$  angle is still computed with respect to the centre of the region (Fig. 6b).

In the present section we introduce a relaxation of the target location in order to produce a smoother trajectory (e.g. Fig. 6c).

## 4.1 Tolerance Management vs. Region Goal

The relaxation introduced by the concept of *region goal* goes beyond the basic exploitation of the position tolerance in the standard funnelling algorithm. Let us recall that standard approach first; in that context, whenever the current location of the mobile entity appears to lie within the circle defined by the position tolerance, the control does not care anymore about the position control but focus only on completing the desired orientation [B05a]. This explains why in Fig 6a the mobile entity does not always achieve *simultaneously* the desired location and the desired orientation. We advocate for adopting such flexible approach as we can always reduce the radius of the position tolerance to enforce a stricter achievement.

Despite the flexibility offered by such a tolerance management, the control is still based on the location of a single point within the tolerance circle, i.e. its centre. This may lead to artificially curved trajectories as illustrated on Fig. 6b. One intuitively understands that, within the tolerance circle, there may exist a better target location for achieving the desired orientation. This is illustrated on Fig. 6c where indeed a different target position induces a smoother trajectory while respecting both the desired position and the orientation tolerances.

Thus the *relaxed funnelling* is based on the concept of *region goal* for which any point belonging to the tolerance circle is eligible to become the target position used for the algorithm described in the previous section. Then two questions arise: how to select such a point within the tolerance circle ? and how do we ensure the stability of such a relaxed steering ?

## 4.2 Selecting the Best Target Position and Ensuring Stability of the Control

### 4.2.1 Principal Criterion

Selecting the best target position means defining an optimality criterion. We have logically adopted the criterion of minimizing the  $|\Delta\eta|$  quantity within the tolerance disk as justified now. This choice derives from the way the standard funnelling control is defined for achieving a desired orientation. Indeed when the desired orientation  $\beta$  matches the  $\eta$  angle then the  $\Delta\eta$  quantity is null and the funnelling control reduces to a simple seek strategy. Our working hypothesis is that such a seek control defines a control cost minima compared to all other cases for which  $|\Delta\eta| > 0$ . So selecting the best target position amounts to find the point(s) within the tolerance circle that minimize  $|\Delta\eta|$  because such a target location minimizes the control cost.

### 4.2.2 Secondary Criterion

The second issue to address is whether multiple optimal points exist in the sense of the above criterion and how to choose the best one among them. Fig. 3 provides hints that indeed there is often a complex subspace of the tolerance region that minimizes the  $|\Delta\eta|$  criterion. As a consequence we have considered an additional secondary criterion of minimizing  $|\alpha|$  that is exploited only for the solutions producing a null  $|\Delta\eta|$ . Minimizing such a secondary criterion corresponds to favor straight line movements over curved movements which is particularly pertinent for producing smooth and short trajectories.

### 4.2.3 Restricted Search of the Optimal Relaxed Direction

Even the two-levels criterion outlined above may produce multiple optimal solution, e.g. when the tolerance region lies in front of the mobile entity. For this reason, and with the additional requirement of minimizing the search computing cost, we have retained to restrict the search to the arc  $\mathcal{A} = [\alpha_{min}, \alpha_{max}]$  defined as the intersection of the position tolerance disk with the sampled arc of radius nearest to the disk centre. Fig. 4 displays the full nearest ring for a few states along a given trajectory towards an oriented goal (only the vectors built from the sampled  $\alpha + \eta$  quantity are displayed, hence their number is reduced for a distant target as visible on Fig. 3a).

### 4.2.4 Determining the Optimal Relaxed Direction $\alpha_r$

The second major working hypothesis for determining the optimal relaxed direction is the monotonous variation of  $(\alpha + \eta)$  over the whole restricted arc  $\mathcal{A}$  even if it crosses 0; by construction the relaxed steering handles only cases with  $\mathcal{A}$  included within  $[-\pi, +\pi]$ .

This hypothesis ensures that we have a monotonous span of final orientation  $\mathcal{F} = [\alpha_{min} + \eta(\alpha_{min}), \alpha_{max} + \eta(\alpha_{max})]$  over the restricted arc  $\mathcal{A}$ . The interval  $\mathcal{F}$  itself may spread beyond  $[-\pi, +\pi]$ . The relaxed steering algorithm then boils down to find the angle  $\alpha_r$  within  $\mathcal{A}$  that minimizes the two-levels criterion described above between  $\mathcal{F}$  and the desired orientation tolerance interval  $\mathcal{T}$ . The pseudo-code is given in Fig. 7.

```

if the centre of  $\mathcal{F}$  and  $\mathcal{T}$  have opposite signs
  if  $\mathcal{F}$  and  $\mathcal{T}$  overlap partially
     $\Delta\eta=0, \alpha_r = 0, \mathbf{End}$ 
  else
    Determine  $\{\{\text{overlap}\}, \{\text{gap}\}\}$  for  $\{\mathcal{F}, \mathcal{T}, (\mathcal{T} +/- 2\pi)\}$ 
    end_if
else //the centre of  $\mathcal{F}$  and  $\mathcal{T}$  have the same sign
  if one boundary of  $\mathcal{F}$  and of  $\mathcal{T}$  have the opposite sign
     $\Delta\eta=0, \alpha_r = 0, \mathbf{End}$ 
  else
    Determine  $\{\{\text{overlap}\}, \{\text{gap}\}\}$  for  $\{\mathcal{F}, \mathcal{T}\}$ 
    end_if
end_if
if some overlap exist
   $\Delta\eta= 0,$ 
   $\alpha_r =$  mapped  $\mathcal{A}$  value of the smallest |overlap boundary|
else
   $\Delta\eta=$  smallest gap between  $\mathcal{F}$  and other intervals
   $\alpha_r =$   $\mathcal{A}$  boundary of the smallest |gap|
end_if
End

```

Fig. 7. Pseudo-code for determining the optimal relaxed direction  $\alpha_r$

The algorithm complexity is independent from the size of the intervals as we check only the boundaries (owing to the monotony hypothesis). This makes the relaxed steering computing cost similar to the one of the standard funnelling. We choose to reduce the cost of evaluating the two  $\eta$  values for  $\mathcal{A}$  boundaries by performing a simple linear interpolation from the table instead of a quintic linear one.

### 4.3 Two Examples

Figure 8 illustrates how the case of Fig6b is treated with the relaxed funnelling algorithm ; the modulated heading direction  $\gamma$  is constructed with respect to the relaxed direction  $\alpha_r$  (to be compared with the standard radial direction  $\alpha$  also shown).

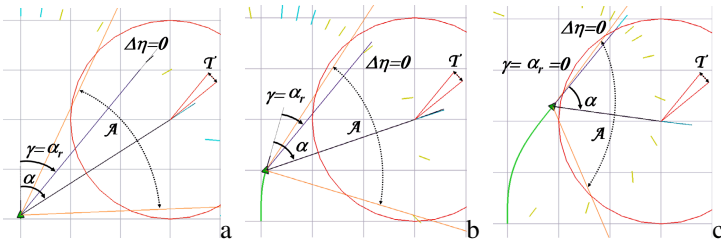


Fig. 8. The relaxed funnelling minimizes  $|\Delta\eta|$ , and  $|\alpha_r|$  in case  $\Delta\eta$  is null

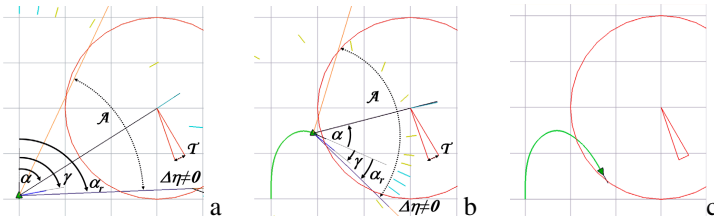


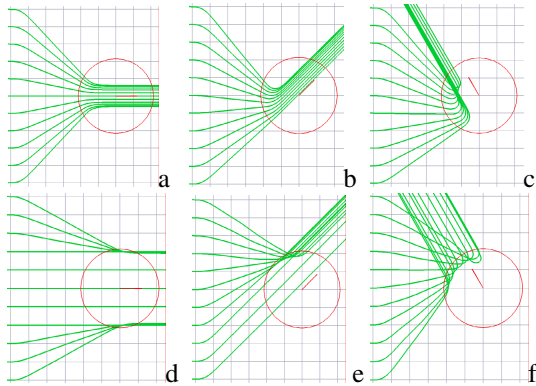
Fig. 9.  $\Delta\eta$  is not null so only the  $|\Delta\eta|$  minimization criterion is exploited to determine  $\alpha_r$

Figure 9 illustrates a more difficult case for which no relaxed direction can produce a null  $\Delta\eta$ . In that case the boundary of  $\mathcal{A}$  minimizing  $|\Delta\eta|$  is retained for  $\alpha_r$ .

## 5 Trajectory Comparison

We present the trajectories obtained for the standard funnelling and the relaxed version introduced in this paper for the same set of moving entities, oriented targets and tolerances. Fig. 10,11, and 12 all show the resulting movement for nine mobile entities starting on the left side of the figures with an initial horizontal orientation. Fig. 10a,b,c are obtained with the standard funnelling whereas Fig.10 d,e,f are obtained with the optimal relaxed direction. The target is defined by the tolerance disk with a desired orientation indicated by the needle in the centre. Once the target is reached the

mobile entities continues their path towards the next target (it was set as much as possible in the same direction as the desired orientation). The comparison of a with d, b with e, and c with f clearly show that the relaxed steering produces less curved trajectories for the same mobile entities. The traveled distance also appears to be frequently smaller.



**Fig. 10.** Trajectories produced by the standard funnelling (top row) and the relaxed funnelling (bottom row) for the same initial conditions: nine mobile entities enters the image from the left side ; they all have the same position goal visible with a large tolerance circle of about 2m radius with a prescribed orientation indicated by a pin shape( a & d: 0°, b & e:45°, c & f:120°). After reaching this goal they all have the same distant goal (not visible).

Fig. 11 highlights that the orientation tolerance is mostly beneficial to the relaxed steering approach. Fig. 12 links multiple successive oriented targets. The relaxed steering appears to produce a globally smoother and shorter path.

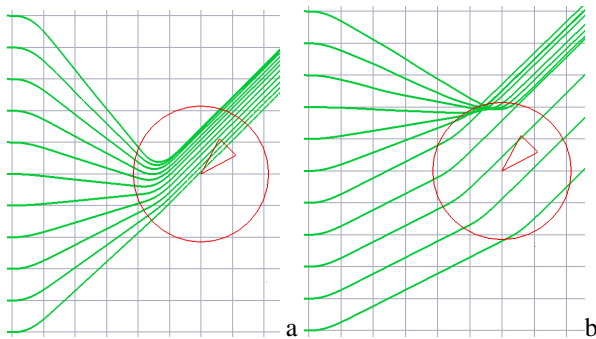


**Fig. 11.** Increasing the orientation tolerance has a minor impact on the trajectories produced with the standard funnelling (a) compared to the much wider spread of trajectories achieved with the relaxed one (b).

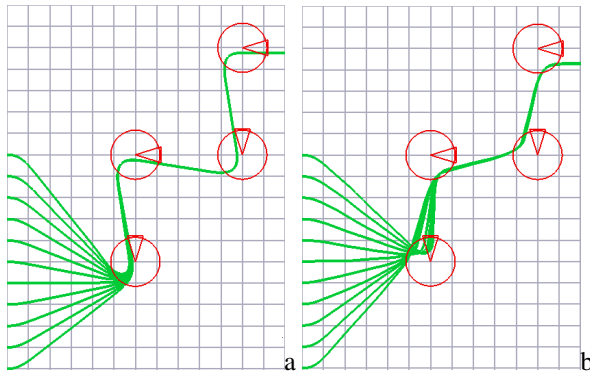


**Fig. 12.** Successive goals highlights the longer and more curved path produced by the standard funnelling (a) compared to the more globally smoother and shorter one obtained with the relaxed algorithm (b). Note too the tendency of trajectories to converge to a single path independently of the initial conditions.

## 7 Performances and Conclusion

The funnelling control update cost (i.e. per frame) is almost independent of the goal parameters. Measurements have been performed on an IBM Thinkpad T60 with Intel Centrino Duo, 1.83 GHz. The computing costs (without display) are reported in Table 1 for the release executable code produced with Microsoft VS 2005 (the algorithm implementation can still be improved). Average values have been computed over roughly 100000 iterations of each algorithm.

**Table 1.** [min, max] measured average computing costs of one funnelling control update in  $\mu\text{s}$  (with the corresponding frequency in KHz) for a large range of oriented goal parameters

	Small tolerances (0.1m and $1^\circ$ ).	Large tolerances (2.5m and $15^\circ$ )
Standard funnelling [B05]	[11 $\mu\text{s}$ , 38 $\mu\text{s}$ ] (90 KHz, 26 KHz)	[20 $\mu\text{s}$ , 39 $\mu\text{s}$ ] (50 KHz, 25 KHz)
Relaxed funnelling	[15 $\mu\text{s}$ , 26 $\mu\text{s}$ ] (67 KHz, 38 KHz)	[8 $\mu\text{s}$ , 26 $\mu\text{s}$ ] (125 KHz, 38 KHz)

Table 1 highlights that the standard and the relaxed funnelling costs do not differ significantly when small position and orientation tolerances are used (an example of application of such a context is handling precise interactions with objects of the environment). On the other hand the relaxed funnelling tends to be on average 50% cheaper for large tolerances typical of outdoor wandering with no precise path to

follow. As a side note, the animation files that are visible on the associated web site (<http://vrlab.epfl.ch/~boulic/Steering/index.html>) have been slowed down for easing the understanding of the algorithm.

By construction the relaxed funnelling can smoothly integrate standard collision avoidance approaches by adding the heading direction modulation induced by the collision avoidance to the one resulting from the funnelling (either standard or relaxed). In case the contribution due to the collision avoidance pushes the mobile entity away from its goal, the relaxed funnelling is able to dynamically adjust the optimal relaxed direction within  $\mathcal{A}$  at the next frame.

To conclude, we have presented the relaxed steering that monitors whether an easier to reach goal exists within the tolerance region and maintain always the easiest to reach goal direction. Its relatively low cost make it a good candidate for handling a large number of moving entities in a dynamically changing environment. Future work will first evaluate the performance of the relaxed steering when combined with collision detection and avoidance. We also plan to introduce the possibility to handle lateral displacements within the general steering approach.

## Acknowledgements

Thanks to Achille Peternier for the MVisio viewer.

## References

- [ALHB06] Arechavaleta, G., Laumond, J.-P., Hicheur, H., Berthoz, A.: Optimizing principles underlying the shape of trajectories in goal oriented locomotion for humans. In: 6th IEEE-RAS International Conference on Humanoid Robots, pp. 131–136, December 4-6 (2006)
- [BOM03] Ben Amor, H., Obst O., Murray, J.: Fast, Neat and Under Control: Inverse Steering Behaviors for Physical Autonomous Agents, Research Report, Institut für Informatik, Universität Koblenz-Landau (December 2003)
- [B05a] Boulic, R.: Proactive Steering Toward Oriented Targets. In: Proceedings of Eurographics 2005 Short Presentations, Dublin (2005)
- [B05b] Boulic, R.: Reaching Oriented Targets with Funnelling Trajectories. In: Proc. of V-CROWDS 2005, Lausanne, November 24-25 (2005) ISBN 10 2-8399-0118-8
- [BJ03] Brogan, D.C., Johnson, N.L.: Realistic Human Walking Paths. In: Proc. of Computer Animation and Social Agents, pp. 94–101 (2003)
- [GKKO08] Geraerts, R., Kamphuis, A., Karamouzas, I., Overmars, M.: Using the Corridor Map Method for Path Planning for a Large Number of Characters. In: Egges, A., Kamphuis, A., Overmars, M. (eds.) MIG 2008. LNCS, vol. 5277, pp. 11–22. Springer, Heidelberg (2008)
- [GTK04] Go, J., Thuc, V., Kuffner, J.J.: Autonomous Behaviors For Interactive Vehicle Animations. In: Proc. of Eurographics/ACM SIGGRAPH Symposium on Computer Animation, pp. 9–18 (2004)
- [HM95] Helbings, D., Molnar, P.C.: Social force model for pedestrian dynamics. *Physical Review E* 51(5), 4282–4286 (1995)
- [LD04] Lamarche, F., Donikian, S.: Crowds of Virtual Humans: a New Approach for Real Time Navigation in Complex and Structured Environments. *Computer Graphics Forum*, 23(3) (2004); In: Eurographics 2004

- [MH04] Metoyer, R.A., Hodgins, J.K.: Reactive Pedestrian Navigation from Examples. *The Visual Computer* 20(10), 635–649 (2004)
- [P08] Pettré, J.: Populate your Game Scene. In: Egges, A., Kamphuis, A., Overmars, M. (eds.) MIG 2008. LNCS, vol. 5277, pp. 33–42. Springer, Heidelberg (2008)
- [PPD07] Paris, S., Pettré, J., Donikian, S.: Pedestrian Reactive Navigation for Crowd Simulation: a Predictive Approach, *Computer Graphics Forum*. In: Eurographics 2007, vol. 26(3), pp. 665–674 (2007)
- [PVT08] Peternier, A., Vexo, F., Thalmann, D.: The Mental Vision framework: a platform for teaching, practicing and researching with Computer Graphics and Virtual Reality. *Transactions on Edutainment 1* (June 2008)
- [RT01] Raupp Musse, S., Thalmann, D.: Hierarchical Model for Real Time Simulation of Virtual Human Crowds. *IEEE Transactions on Visualization and Computer Graphics* 7(2), 152–164 (2001)
- [R99] Reynolds, C.W.: Steering Behaviors For Autonomous Characters. In: Proc. 1999 Game Developer's Conference, pp. 763–782 (1999)
- [R00] Reynolds, C.W.: Interaction with Groups of Autonomous Characters. In: Proc. 1999 Game Developer's Conference (2000)
- [SNKFR08] Singh, S., Naik, M., Kapadia, M., Faloutsos, P., Reinman, G.: Watch Out! A Framework for Evaluating Steering Behaviors. In: Egges, A., Kamphuis, A., Overmars, M. (eds.) MIG 2008. LNCS, vol. 5277, pp. 200–209. Springer, Heidelberg (2008)